

DYNAMICS OF A CONTROLLED ANTI-AIRCRAFT MISSILE LAUNCHER MOUNTED ON A MOVEABLE BASE

ZBIGNIEW KORUBA
ZBIGNIEW DZIOPA
IZABELA KRZYSZTOFIK

*Kielce University of Technology, Faculty of Mechatronics and Machine Building, Kielce, Poland
e-mail: ksmzko@tu.kielce.pl; zdziopa@tu.kielce.pl; pssik@tu.kielce.pl*

In the work, dynamics of a controlled anti-aircraft missile launcher mounted on a moveable base (wheeled vehicle) is analysed. Pre-programmed controls were used for basic motion of the launcher during target interception, and stabilizing controls were applied to counteract disturbances resulting from the operation of the anti-aircraft system. This type of control allows setting the longitudinal axis of the missile with respect to the target line of sight irrespective of the carrier vehicle motion. The system vibrations are due to road-induced excitations and they act directly on the vehicle, the missile launch and the control of launcher basic motion. Selected results of computer simulation were presented graphically.

Key words: dynamics, control, launcher, missile

1. Introduction

Modern self-propelled anti-aircraft missile systems with short-range self-guided missiles should be able to detect, identify and track aerial targets when the launcher-carrier vehicles are in motion. To improve the system accuracy, it is necessary to apply pre-programmed controls for target detection and corrective controls for target tracking (Dziopa, 2004, 2005, 2006a; Koruba, 2001; Koruba and Osiecki, 1999).

Synthesis of the launcher control involves determination the impact that road-induced kinematic excitations may have on the launcher performance. It is desirable that any transitional process accompanying terrain unevenness (a bump) be optimally attenuated.

In this paper, motion of a launcher-missile system was considered in a three-dimensional Euclidean space and Earth's gravitational field. There were

six degrees of freedom in the discrete model of the system described by analytical relations in the form of equations of motion, kinematic relations and three equations of equilibrium (Dziopa, 2006b,c).

In the general case, a launcher-missile system is not symmetric about the longitudinal vertical plane going through the centre of the system mass (Dziopa, 2008; Mishin, 1990; Mitschke, 1972; Svetlitskiy, 1963). The symmetry refers to selected geometrical dimensions and properties of flexible elements. In the general case, the inertial characteristic departs from this symmetry. The launcher turret can rotate with respect to the carrier together with the guide rail and the missile. The turret rotates in accordance with the azimuth angle ψ_{pv} , which is the turret yaw angle. The turret and the guide rail mounted on it constitute a rotary kinematic pair. The guide rail can rotate with respect to the turret in accordance with the elevation angle ϑ_{pv} , which is the guide rail pitch angle. This leads to an asymmetric distribution of masses. The system is reduced to a structural discrete model describing the phenomena that are mechanical excitations in character. The basic motion of the turret is reduced to basic motion of the carrier. The turret is an object whose inertial characteristic is dependent on the position of the target with respect to the anti-aircraft system. The mass of the turret remains constant, but its moments of inertia and moments of deviation change.

The launcher was modelled as two basic masses, four deformable elements and a control system, as shown schematically in Fig. 1.

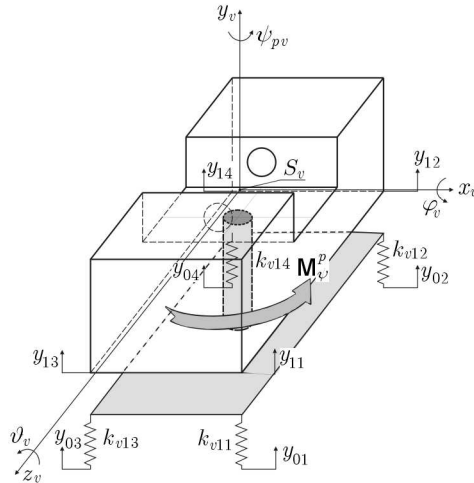


Fig. 1. Physical model of the controlled launcher

The launcher is a perfectly stiff body with mass m_v , moments of inertia I_{vx} , I_{vy} and I_{vz} and a moment of deviation I_{vxxz} . The launcher is mounted on the vehicle using four passive elastic-attenuating elements with linear parameters k_{v11} and c_{v11} , k_{v12} and c_{v12} , k_{v13} and c_{v13} as well as k_{v14} and c_{v14} , respectively.

The turret is a perfectly stiff body with mass m_w and main central moments of inertia $I_{w\xi'_v}$, $I_{w\eta'_v}$, $I_{w\zeta'_v}$. The guide rail is also a perfectly stiff body with mass m_{pr} and main central moments of inertia $I_{pr\xi_{pv}}$, $I_{pr\eta_{pv}}$, $I_{pr\zeta_{pv}}$.

If the basic motion of the launcher is not disturbed, then the $0_vx_vy_vz_v$, $S_vx_vy_vz_v$ and $S_v\xi_v\eta_v\zeta_v$ coordinate systems coincide at any moment. The turret model as an element of the spatially vibrating system performs complex motion with respect to the $0_vx_vy_vz_v$ reference system consisting of straightline motion of the mass centre S_v , in accordance with a change in the y_v coordinate, rotary motion about the S_vz_v axis in accordance with a change in the pitch angle ϑ_v and rotary motion about the S_vx_v axis in accordance with a change in the tilt angle φ_v .

Prior to the launch, the missile is rigidly connected with the guide rail. The mounting prevents the missile from moving along the guide rail. Once the missile motor is activated, the missile moves along the rail.

The guide rail-missile system used in the analysis ensures collinearity of points on the missile and the guide rail.

It is assumed that the longitudinal axis of the missile coincides with the longitudinal axis of the guide rail at any moment and that the missile is a stiff body with an unchangeable characteristic of inertia. The missile is a perfectly stiff body with mass m_p and main central moments of inertia I_{px_p} , I_{py_p} , I_{pz_p} . The geometric characteristic of the guide rail-missile system shown in Fig. 2a and Fig. 2b can be used to analyze the dynamics of the controlled system.

The main view of the turret-missile system model is presented in Fig. 2a. It includes an instantaneous position of the missile while it moves along the guide rail. Figure 2b shows the top view of the turret-missile system model. It includes the instantaneous position of the missile while it moves along the guide rail.

The missile model performs straightline motion with respect to the $S_v\xi_{pv}\eta_{pv}\zeta_{pv}$ reference system according to a change in the ξ_{pv} coordinate.

The model of the launcher-missile system has six degrees of freedom, which results from the structure of the formulated model. The positions of the system were determined at any moment assuming four independent generalized coordinates:

y_v – vertical displacement of the turret mass centre S_v ,
 φ_v – angle of rotation of the turret about the $S_v x_v$ axis,
 ϑ_v – angle of rotation of the turret about the $S_v z_v$ axis,
 ξ_{pv} – straightline displacement of the missile mass centre S_p along the $S_v \xi_{pv}$ axis.

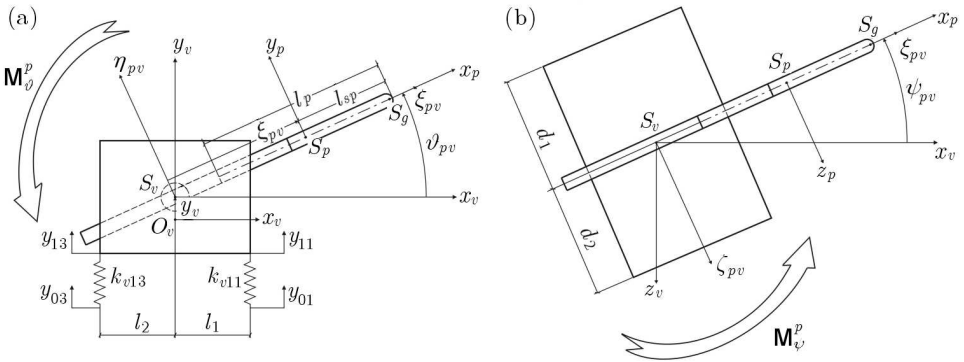


Fig. 2. (a) Side view of the turret-and-missile model; (b) top view of the turret-and-missile model

2. Model of motion of the launcher on a moveable base

The mathematical model of the system was developed basing on the physical model. Six independent generalized coordinates were selected to determine the kinetic and potential energy of the model and the distribution of generalized forces basing on the considerations for the physical model. By using the second order Lagrange equations, it was possible to derive equations of motion of the analysed system. The system was reduced to a structural discrete model, which required applying differential equations with ordinary derivatives.

Six independent coordinates were used to determine motion of the launcher-missile system model:

- turret vibrations: $y_v, \vartheta_v, \varphi_v$,
- basic motion of the turret and the guide rail ψ_{pv} and ϑ_{pv} , respectively,
- missile motion with respect to the guide rail ξ_{pv} .

Motion of the controlled launcher mounted on a moveable base can be illustrated by means of the following equations

$$\begin{aligned}
 \ddot{\vartheta}_v &= \frac{1}{b_7}[z_2 - (b_2\ddot{y}_v + b_8\ddot{\varphi}_v + b_9\ddot{\xi}_{pv} + b_{10}\ddot{\psi}_{pv} + b_{11}\ddot{\vartheta}_{pv})] + M_{\vartheta} \\
 \ddot{\varphi}_v &= \frac{1}{b_{12}}[z_3 - (b_3\ddot{y}_v + b_8\ddot{\vartheta}_v + b_{13}\ddot{\xi}_{pv} + b_{14}\ddot{\psi}_{pv} + b_{15}\ddot{\vartheta}_{pv})] + M_{\varphi} \\
 \ddot{y}_v &= \frac{1}{b_1}[z_1 - (b_2\ddot{\vartheta}_v + b_3\ddot{\varphi}_v + b_4\ddot{\xi}_{pv} + b_5\ddot{\psi}_{pv} + b_6\ddot{\vartheta}_{pv})] + F_y \\
 \ddot{\psi}_{pv} &= \frac{1}{b_{19}}[z_5 - (b_5\ddot{y}_v + b_{10}\ddot{\vartheta}_v + b_{14}\ddot{\varphi}_v + b_{17}\ddot{\xi}_{pv} + b_{20}\ddot{\vartheta}_{pv})] + M_{\psi}^p \\
 \ddot{\vartheta}_{pv} &= \frac{1}{b_{21}}[z_6 - (b_6\ddot{y}_v + b_{11}\ddot{\vartheta}_v + b_{15}\ddot{\varphi}_v + b_{18}\ddot{\xi}_{pv} + b_{20}\ddot{\psi}_{pv})] + M_{\vartheta}^p \\
 \ddot{\xi}_{pv} &= \frac{1}{b_{16}}[z_4 - (b_4\ddot{y}_v + b_9\ddot{\vartheta}_v + b_{13}\ddot{\varphi}_v + b_{17}\ddot{\psi}_{pv} + b_{18}\ddot{\vartheta}_{pv})]
 \end{aligned} \tag{2.1}$$

where

y_v – vertical displacement of the turret mass centre S_v ,

φ_v, ϑ_v – angle of rotation of the turret about the $S_v x_v$ and $S_v z_v$ axis, respectively,

ξ_{pv} – straightline displacement of the missile mass centre S_p along the $S_v \xi_{pv}$ axis,

ψ_{pv} – turret yaw angle,

ϑ_{pv} – guide rail pitch angle,

$M_{\vartheta}^p, M_{\psi}^p$ – preprogrammed moment of control of the turret pitch angle and the guide rail yaw angle, respectively,

F_y – force stabilizing vertical progressive motion of the launcher,

$M_{\vartheta}, M_{\varphi}$ – moments stabilizing angular motions of the launcher about the $S_v z_v$ and $S_v x_v$ axes,

b_i (where $i = 1, \dots, 21$) – coordinate functions $y_v, \vartheta_v, \varphi_v, \psi_{pv}, \vartheta_{pv}, \xi_{pv}$,

z_i (where $i = 1, \dots, 6$) – coordinate functions $y_v, \vartheta_v, \varphi_v, \psi_{pv}, \vartheta_{pv}, \xi_{pv}$ and their derivatives with respect to time $\dot{y}_v, \dot{\vartheta}_v, \dot{\varphi}_v, \dot{\psi}_{pv}, \dot{\vartheta}_{pv}, \dot{\xi}_{pv}$.

Explicit forms of the functions $b_i(y_v, \vartheta_v, \varphi_v, \psi_{pv}, \vartheta_{pv}, \xi_{pv})$ and $z_i(y_v, \vartheta_v, \varphi_v, \psi_{pv}, \vartheta_{pv}, \xi_{pv}, \dot{y}_v, \dot{\vartheta}_v, \dot{\varphi}_v, \dot{\psi}_{pv}, \dot{\vartheta}_{pv}, \dot{\xi}_{pv})$ are long mathematical expressions, which developed analytically are available at the authors of the article.

3. Control of motion of the launcher on a moveable base

The launcher under consideration is mounted on a moveable base (wheeled vehicle). It can be put into rotary motion by angle ψ_{pv} about the $S_v y_v$ axis and rotary motion by angle ϑ_{pv} about the $S_v z_v$ axis. When the missile longitudinal axis $S_v x_p$ is set, for instance, to coincide with the target line of sight, it is necessary to apply the following pre-programmed control moments of the launcher

$$\begin{aligned} M_{\psi}^p &= k_{pv}^{\psi}(\psi_{pv} - \psi_{pv}^p) + c_{pv}^{\psi}(\dot{\psi}_{pv} - \dot{\psi}_{pv}^p) \\ M_{\vartheta}^p &= k_{pv}^{\vartheta}(\vartheta_{pv} - \vartheta_{pv}^p) + c_{pv}^{\vartheta}(\dot{\vartheta}_{pv} - \dot{\vartheta}_{pv}^p) \end{aligned} \tag{3.1}$$

where

$k_{pv}^{\psi}, k_{pv}^{\vartheta}$ – gain coefficients of the control system,

$c_{pv}^{\psi}, c_{pv}^{\vartheta}$ – attenuation coefficients of the control system.

The principle of operation of the launcher control system is presented in a schematic diagram in Fig. 3.

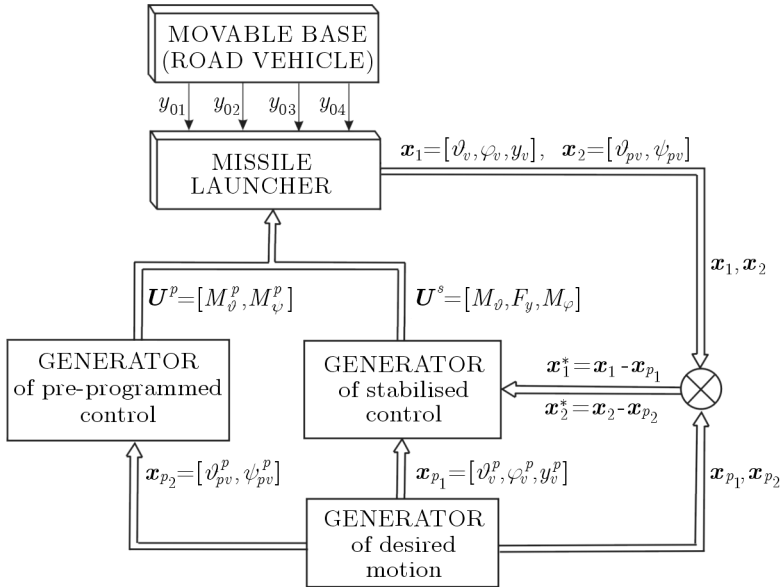


Fig. 3. Diagram of the system for automatic control of the launcher on the moveable base

The quantities ψ_{pv}^p and ϑ_{pv}^p present in the above formulas are pre-programmed angles changing in time according to the following laws

$$\begin{aligned} \psi_{pv}^p &= \omega_{pv}^\psi t & \vartheta_{pv}^p &= \vartheta_{pv0} \sin(\omega_{pv}^\vartheta t + \varphi_{pv0}) \\ \dot{\psi}_{pv}^p &= \omega_{pv}^\psi & \dot{\vartheta}_{pv}^p &= \vartheta_{pv0} \omega_{pv}^\vartheta \cos(\omega_{pv}^\vartheta t + \varphi_{pv0}) \end{aligned} \tag{3.2}$$

where

$$\omega_{pv}^\psi = \frac{2\pi}{T_\psi} \quad \omega_{pv}^\vartheta = \frac{2\pi}{T_\vartheta}$$

Once the launcher is in the pre-determined final state, the longitudinal axis of the guide rail needs to coincide with the target line of sight irrespective of motions of the base or external disturbances.

The stabilizing (corrective) controls used for the automatic control of the launcher need to have the following form

$$\begin{aligned} M_\vartheta &= k_\vartheta(\vartheta_\nu - \vartheta_\nu^p) + c_\vartheta(\dot{\vartheta}_\nu - \dot{\vartheta}_\nu^p) & M_\varphi &= k_\varphi(\varphi_\nu - \varphi_\nu^p) + c_\varphi(\dot{\varphi}_\nu - \dot{\varphi}_\nu^p) \\ F_y &= k_y(y_\nu - y_\nu^p) + c_y(\dot{y}_\nu - \dot{y}_\nu^p) \end{aligned} \tag{3.3}$$

where

$\vartheta_\nu^p, \varphi_\nu^p, y_\nu^p$ – quantities defining the pre-determined position of the launcher in space during angular motions of the base,

$k_\vartheta, k_\varphi, k_y$ – gain coefficients of the regulator,

$c_\vartheta, c_\varphi, c_y$ – attenuation coefficients of the regulator.

4. Results

4.1. System parameters

Motion of the hypothetical controlled anti-aircraft missile launcher was described using the system of equations denoted by (2.1). The launcher system was assumed to have the following parameters:

- Parameters of the launcher (turret and guide rail)

$$\begin{aligned} m_\nu &= m_w + m_{pr} & I_{\nu\eta'_{pv}} &= 7 \text{ kgm}^2 \\ I_{\nu x} &= (I_{w\xi'_\nu} + I_{pr\xi_{pv}} \cos^2 \vartheta_{pv} + I_{pr\eta_{pv}} \sin^2 \vartheta_{pv}) \cos^2 \psi_{pv} + \\ &+ (I_{w\xi'_\nu} + I_{pr\xi_{pv}}) \sin^2 \psi_{pv} \\ I_{\nu y} &= I_{\nu\eta'_{pv}} + I_{pr\xi_{pv}} \cos^2 \vartheta_{pv} + I_{pr\eta_{pv}} \sin^2 \vartheta_{pv} \end{aligned}$$

$$\begin{aligned}
I_{vz} &= (I_w \xi'_v + I_{pr} \xi_{pv} \cos^2 \vartheta_{pv} + I_{pr} \eta_{pv} \sin^2 \vartheta_{pv}) \sin^2 \psi_{pv} + \\
&\quad + (I_w \zeta'_v + I_{pr} \zeta_{pv}) \cos^2 \psi_{pv} \\
I_{vzx} &= (I_w \xi'_v + I_{pr} \xi_{pv} \cos^2 \vartheta_{pv} + I_{pr} \eta_{pv} \sin^2 \vartheta_{pv} - I_w \zeta'_v - I_{pr} \zeta_{pv}) \cdot \\
&\quad \cdot \cos \psi_{pv} \sin \psi_{pv} \\
m_w &= 50 \text{ kg} & I_w \xi'_v &= 10 \text{ kgm}^2 \\
I_w \eta'_v &= 7 \text{ kgm}^2 & I_w \zeta'_v &= 12 \text{ kgm}^2 \\
m_{pr} &= 30 \text{ kg} & I_{pr} \xi_{pv} &= 0.6 \text{ kgm}^2 \\
I_{pr} \eta_{pv} &= 4 \text{ kgm}^2 & I_{pr} \zeta_{pv} &= 3.5 \text{ kgm}^2
\end{aligned}$$

- Launcher suspension parameters

$$\begin{aligned}
k_{v11} &= 30000 \text{ N/m} & c_{v11} &= 150 \text{ Ns/m} \\
k_{v12} &= 30000 \text{ N/m} & c_{v12} &= 150 \text{ Ns/m} \\
k_{v13} &= 30000 \text{ N/m} & c_{v13} &= 150 \text{ Ns/m} \\
k_{v14} &= 30000 \text{ N/m} & c_{v14} &= 150 \text{ Ns/m}
\end{aligned}$$

- Missile parameters

$$\begin{aligned}
m_p &= 12 \text{ kg} & I_{px_p} &= 0.01 \text{ kgm}^2 \\
I_{py_p} &= 2 \text{ kgm}^2 & I_{pz_p} &= 2 \text{ kgm}^2
\end{aligned}$$

- Geometric characteristics

$$\begin{aligned}
l_1 &= 0.3 \text{ m} & l_2 &= 0.3 \text{ m} \\
d_1 &= 0.2 \text{ m} & d_2 &= 0.2 \text{ m} \\
l_p &= 1.6 \text{ m} & l_{sp} &= 0.8 \text{ m}
\end{aligned}$$

- Thrust and operation time of the missile starter motor

$$P_{ss} = 4000 \text{ N} \quad t_{ss} = 0.07 \text{ s}$$

4.2. Kinematic excitations

The terrain unevenness, i.e. a bump, was assumed to be a kinematic excitation. The basic motion of the vehicle carrying the launcher was defined as

$$s_n = V_n(t - t_{gb})$$

where

$V_n = 8.3 \text{ m/s}$ – velocity of the vehicle with the launcher,

$t_{gb} = 0.5 \text{ s}$ – time in which the vehicle carrying the launcher goes over the bump with the front wheels.

In the case considered here, all the vehicle wheels climb a single bump.

The excitations have the following form

$$\begin{aligned} y_{01} &= y_0 \sin^2(\omega_0 s_n) & \dot{y}_{01} &= y_0 \omega_0 V_n \sin(2\omega_0 s_n) \\ y_{02} &= y_0 \sin^2(\omega_0 s_n) & \dot{y}_{02} &= y_0 \omega_0 V_n \sin(2\omega_0 s_n) \\ y_{03} &= y_0 \sin^2[\omega_0(s_n - l_{wn})] & \dot{y}_{03} &= y_0 \omega_0 V_n \sin[2\omega_0(s_n - l_{wn})] \\ y_{04} &= y_0 \sin^2[\omega_0(s_n - l_{wn})] & \dot{y}_{04} &= y_0 \omega_0 V_n \sin[2\omega_0(s_n - l_{wn})] \end{aligned}$$

where $y_0 = 0.05 \text{ m}$, $l_0 = 0.35 \text{ m}$, $\omega_0 = \pi/l_0$, $l_{wn} = l_1 + l_2$.

- Control parameters

$$\begin{array}{lll} T_\psi = 1 \text{ s} & T_\vartheta = 1 \text{ s} & \vartheta_{pv0} = \frac{\pi}{2} \\ \varphi_{pv0} = \frac{\pi}{4} & \text{or} & \varphi_{pv0} = 0 \\ k_\vartheta = 50000 & k_\varphi = 20000 & k_y = 50000 \\ c_\vartheta = 5000 & c_\varphi = 2000 & c_y = 5000 \end{array}$$

— low values of the coefficients of the pre-programmed controls

$$\begin{array}{ll} k_{pv}^\psi = 2000 & k_{pv}^\vartheta = 2000 \\ c_{pv}^\psi = 200 & c_{pv}^\vartheta = 200 \end{array}$$

— high values of the coefficients of the pre-programmed controls

$$\begin{array}{ll} k_{pv}^\psi = 10000 & k_{pv}^\vartheta = 10000 \\ c_{pv}^\psi = 2000 & c_{pv}^\vartheta = 2000 \end{array}$$

Figures 4-21 show selected results of computer simulation conducted for the hypothetical controlled missile launcher.

Figures 5-13 illustrate the performance of the launcher with no or some correction applied to the automatic control system (Figures a and b, respectively) during motion of the vehicle over the uneven terrain (a single road bump). By analogy, the effects of the pre-programmed controls are presented in Figs. 14-21. The low and high coefficients of the control system are shown in Figs. 17-21 a and b, respectively.

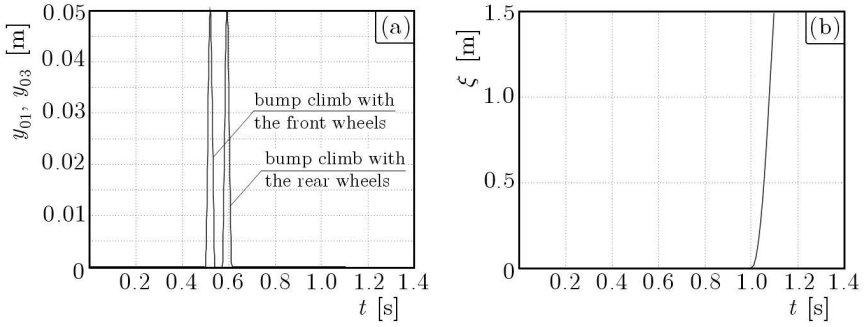


Fig. 4. (a) Time-dependent profile of the terrain unevenness (bump); (b) time-dependent translatory displacements of the rocket with regard to the guide rail

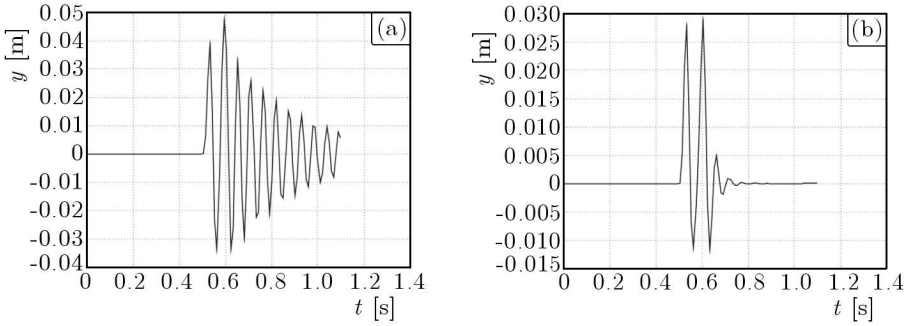


Fig. 5. Time-dependent vertical displacement y of the launcher without (a) and with (b) correction

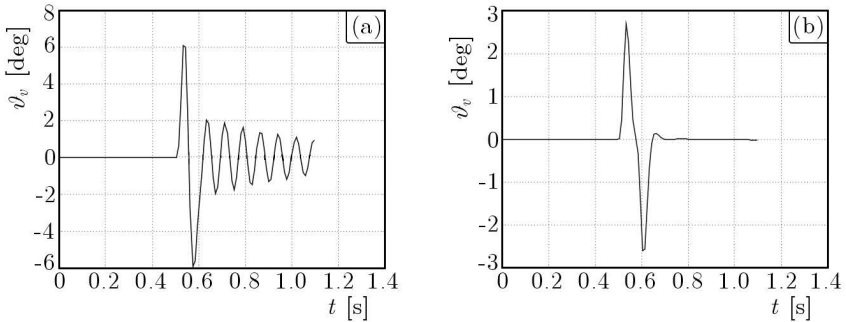


Fig. 6. Time-dependent angular displacement φ_v of the launcher turret without (a) and with (b) correction

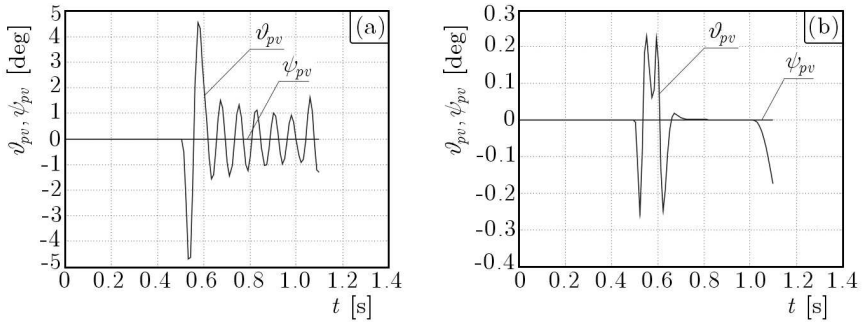


Fig. 7. Time-dependent angular displacements of the launcher without (a) and with (b) correction, ϑ_{pv} and ψ_{pv} , respectively

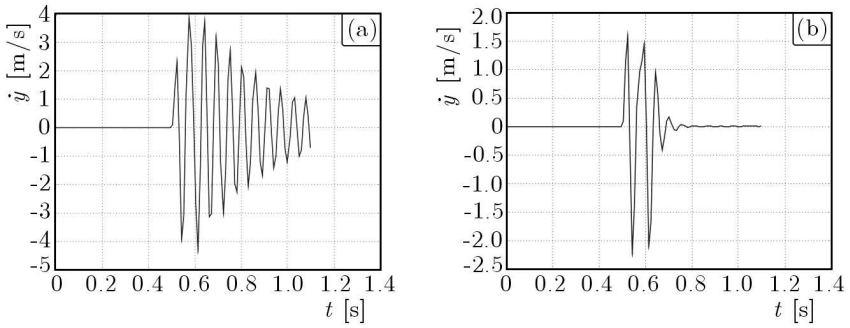


Fig. 8. Time-dependent vertical velocity of the launcher without (a) and with (b) correction, \dot{y}

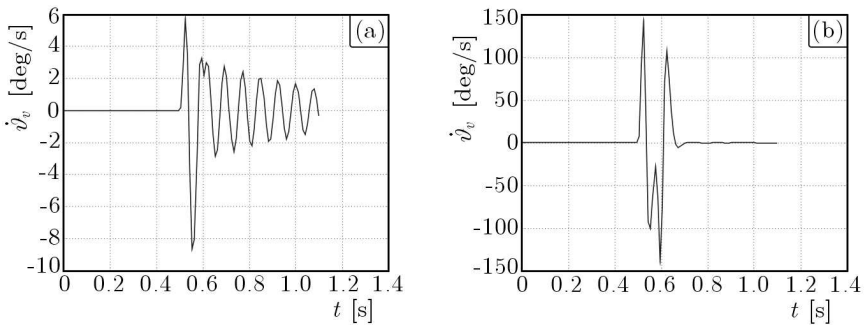


Fig. 9. Time-dependent angular velocity of the launcher turret without (a) and with (b) correction, $\dot{\vartheta}_v$

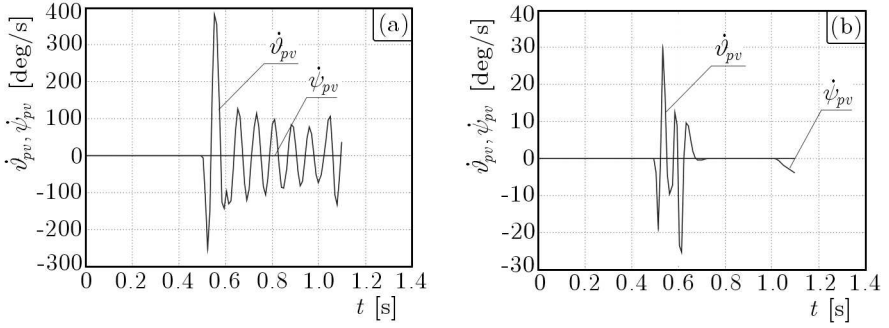


Fig. 10. 11a. Time-dependent angular velocities of the launcher without (a) and with (b) correction, $\dot{\vartheta}_{pv}$ and $\dot{\psi}_{pv}$, respectively

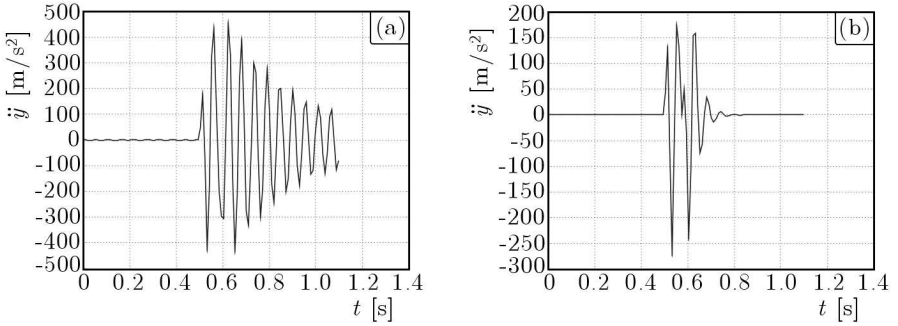


Fig. 11. Time-dependent vertical acceleration of the launcher without (a) and with (b) correction, \ddot{y}

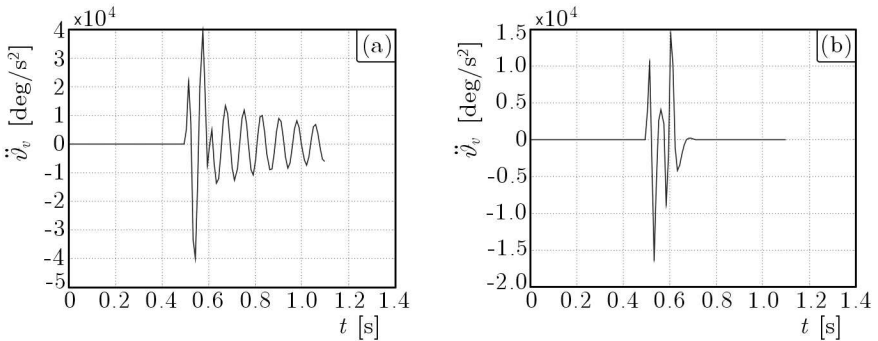


Fig. 12. Time-dependent angular acceleration of the launcher turret without (a) and with (b) correction, $\ddot{\vartheta}_v$

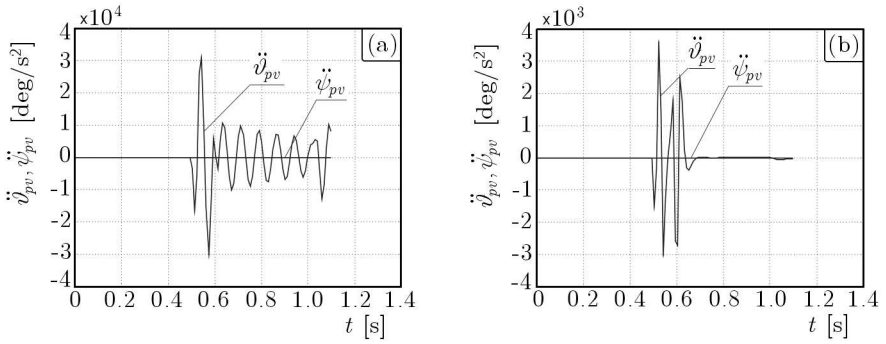


Fig. 13. Time-dependent angular accelerations of the launcher without (a) and with (b) correction, $\ddot{\vartheta}_{pv}$ and $\ddot{\psi}_{pv}$, respectively

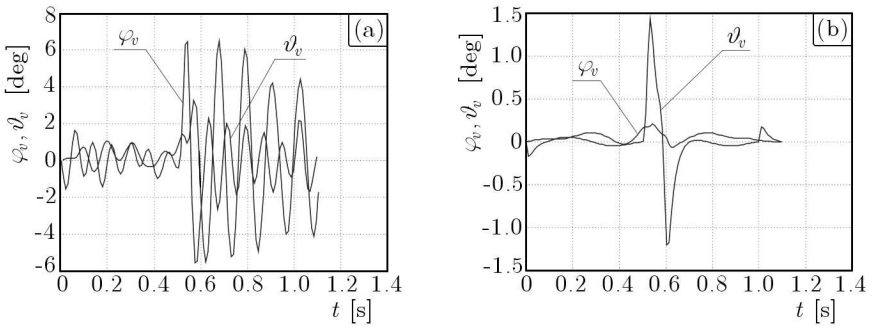


Fig. 14. Time-dependent angular displacements of the launcher turret during pre-programmed control without (a) and with (b) correction, ϑ_v and φ_v , respectively

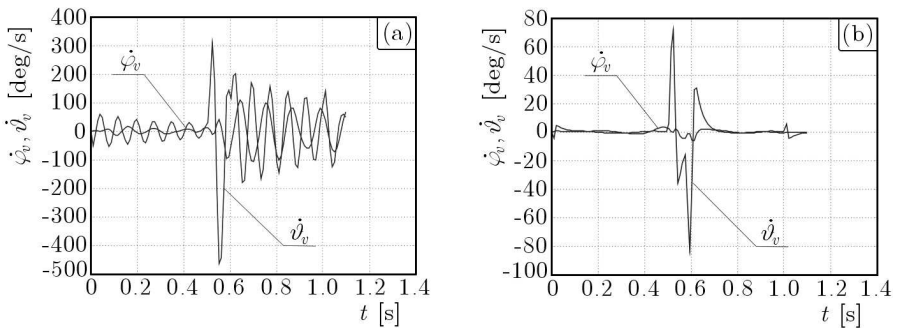


Fig. 15. Time-dependent angular velocities of the launcher turret during pre-programmed control without (a) and with (b) correction, $\dot{\vartheta}_v$ and $\dot{\varphi}_v$, respectively

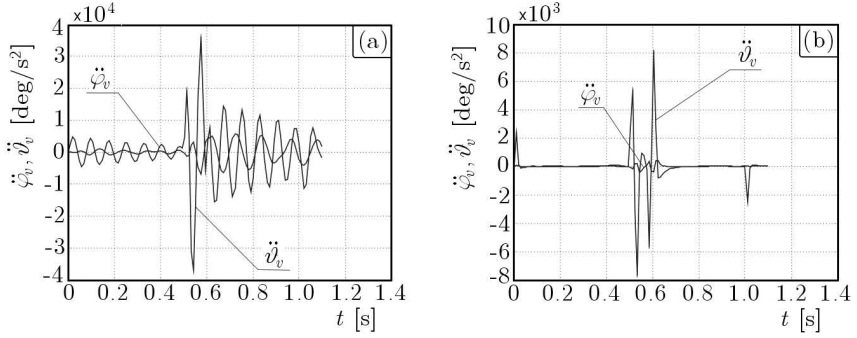


Fig. 16. Time-dependent angular velocities of the launcher turret during pre-programmed control without (a) and with (b) correction, $\ddot{\vartheta}_v$ and $\ddot{\varphi}_v$, respectively

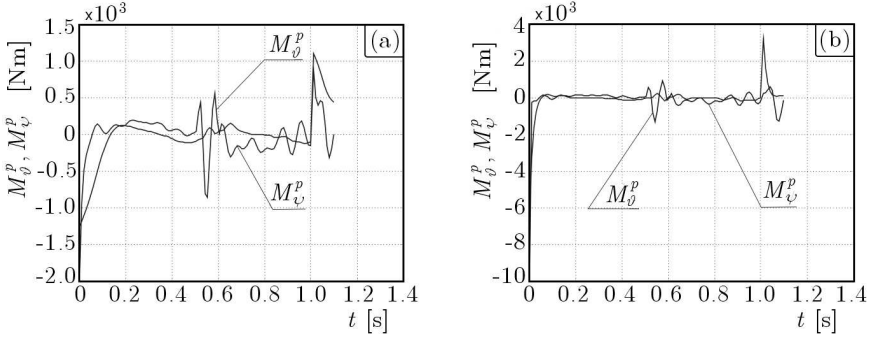


Fig. 17. Time-dependent pre-programmed control moments M_ψ^p and M_φ^p at low (a) and high (b) gain coefficients

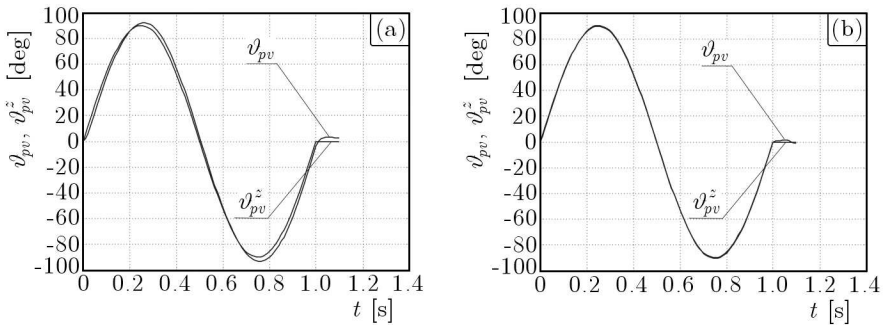


Fig. 18. 19a. Time-dependent pre-determined and real angular pitches of the launcher at low (a) and high (b) gain coefficients, ϑ_{pv}^z and ϑ_{pv} , respectively

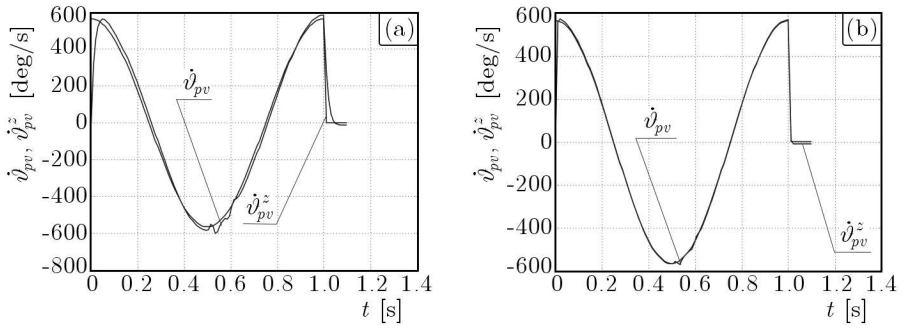


Fig. 19. Time-dependent pre-determined and real angular velocities of the launcher at low (a) and high (b) gain coefficients, $\dot{\psi}_{pv}^z$ and $\dot{\psi}_{pv}$, respectively

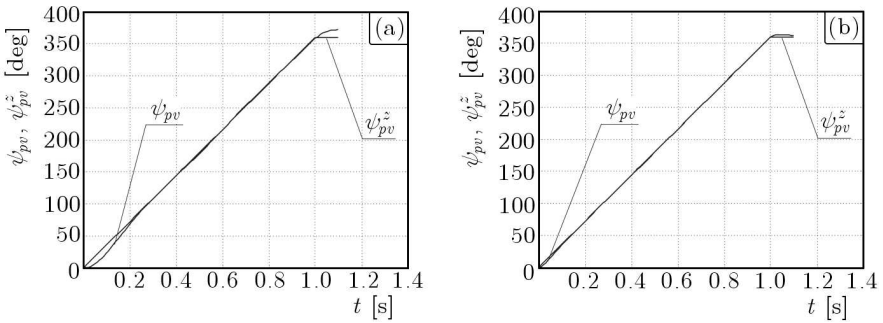


Fig. 20. Time-dependent pre-determined and real angular displacements of the launcher at low (a) and high (b) gain coefficients, ψ_{pv}^z and ψ_{pv} , respectively

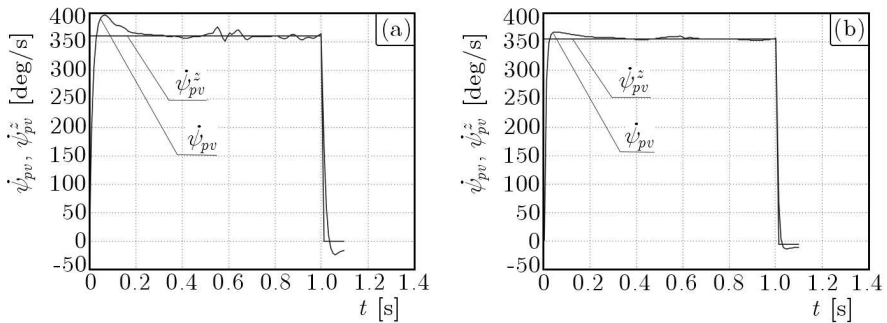


Fig. 21. Time-dependent pre-determined and real angular velocities of the launcher at low (a) and high (b) gain coefficients, $\dot{\psi}_{pv}^z$ and $\dot{\psi}_{pv}$, respectively

5. Conclusions

The following conclusions were drawn from the theoretical considerations and simulation tests:

- corrective controls must to be applied to prevent the occurrence of transitional processes resulting from terrain unevenness conditions (bumps);
- pre-programmed controls of the launcher result in negative vibrations of all its elements; the vibrations can be removed effectively by optimal selection of the coefficients of gain and attenuation in the launcher control system;
- the launcher control system allows immediate positioning of the launcher in space so that the guide-rail longitudinal axis coincides with the target line of sight.

A feasibility study should to be conducted for the proposed control system. Particular attention has to be paid to values of the pre-programmed and corrective control moments.

References

1. DZIOPA Z., 2004, The dynamics of a rocket launcher placed on a self-propelled vehicle, *Mechanical Engineering*, **91**, 3, ISSN 1729-959, 23-30, Lviv
2. DZIOPA Z., 2005, An analysis of physical phenomena generated during the launch of a missile from an anti-aircraft system, *The Prospects and Development of Rescue, Safety and Defense Systems in the 21st Century*, Polish Naval Academy, Gdynia, ISBN 83-87280-78-X, 296-303
3. DZIOPA Z., 2006a, An anti-aircraft self-propelled system as a system determining the initial parameters of the missile flight, *Mechanics in Aviation ML-XII 2006*, PTMTS, Warsaw, ISBN 83-902194-6-8, 223-241
4. DZIOPA Z. 2006b, Modelling an anti-aircraft missile launcher mounted on a road vehicle, *Theory of Machines and Mechanisms*, Vol. 1, University of Zielona Góra and PKTMiM, ISBN 83-7481-043-2, 205-210
5. DZIOPA Z., 2006c, The missile coordinator system as one of the objects of an anti-aircraft system, *6th International Conference on Armament Technology: Scientific Aspects of Armament Technology*, Waplewo, Military University of Technology, ISBN 83-89399-27-X, 221-229

6. DZIOPA Z., 2008, *The Modelling and Investigation of the Dynamic Properties of the Sel-Propelled Anti-Aircraft System*, Published by Kielce University of Technology, Kielce
7. KORUBA Z., 2001, *Dynamics and Control of a Gyroscope on Board of an Flying Vehicle*, Monographs, Studies, Dissertations No. 25, Kielce University of Technology, Kielce [in Polish]
8. KORUBA Z., DZIOPA Z., KRZYSZTOFIK I., 2009, Dynamics and control of a gyroscope-stabilized platform in a self-propelled anti-aircraft system, *Journal of Theoretical and Applied Mechanics*, **48**, 1, 5-26
9. KORUBA Z., OSIECKI J., 1999, *Construction, Dynamics and Navigation of Close-Range Missiles – Part 1*, University Course Book No. 348, Kielce University of Technology Publishing House, PL ISSN 0239-6386 [in Polish]
10. KORUBA Z., TUŚNIO J., 2009, A gyroscope-based system for locating a point source of low-frequency electromagnetic radiation, *Journal of Theoretical and Applied Mechanics*, **47**, 2, 343-362
11. MISHIN B.P., 1990, *Dinamika raket*, Mashinostroyeniye, Moskva
12. MITSCHKE M., 1977, *Dynamics of a Motor Vehicle*, WKŁ, Warszawa [in Polish]
13. SVIETLITSKIY V.A., 1963, *Dinamika starta letatelnykh apparatov*, Nauka, Moskva

Dynamika sterowanej przeciwlotniczej wyrzutni raketowej umieszczonej na ruchomej platformie

Streszczenie

W pracy dokonano analizy dynamiki sterowanej przeciwlotniczej wyrzutni pocisków raketowych umieszczonej na ruchomej podstawie (pojeździe samochodowym). Zastosowano sterowanie programowe dla ruchu podstawowego wyrzutni realizowanego w procesie przechwytywania celu oraz sterowanie stabilizujące zaburzenia wynikające z działania zestawu przeciwlotniczego. Tego rodzaju sterowanie pozwala na ustawienie osi podłużnej pocisku raketowego względem linii obserwacji celu niezależnie od ruchu pojazdu, na którym znajduje się wyrzutnia. Drgania spowodowane są wymuszeniami działającymi bezpośrednio na pojazd samochodowy od strony drogi, startem pocisku raketowego oraz sterowanego ruchu podstawowego samej wyrzutni. Niektóre wyniki badań symulacji komputerowej przedstawione są w graficznej postaci.

Manuscript received May 14, 2009; accepted for print June 19, 2009